Synthetic peptides as tools in chemical immunology

Doelman, W.

3

Citrullinated human and murine MOG_{35-55} display distinct biophysical and biochemical behavior

W. Doelman, R.C. Reijnen, N. van Driel, I. Philippens, S.I. van Kasteren and M.C. Araman contributed to the work presented in this chapter

Introduction

Multiple Sclerosis (MS) is a family of neurodegenerative autoimmune diseases that presents itself pathologically in the form of neuroinflammation, demyelination and axonal damage.[1] Most patients (±85%) start with the remitting-relapsing form of the disease (RRMS), where episodes of neurological impairment (relapse) are followed by periods of symptom free survival (remission). A large cohort (±60%) of these patients later progresses into secondary progressive MS (SPMS), where neurological damage is chronic. A small portion of the patients

(10-15%) starts off with a progressive form of the disease. This is called primary progressive MS (PPMS).[2] While treatments exist to manage the remitting form of the disease, the progressive forms are untreatable at present.[3]

While involvement of the immune system is well established, the critical autoantigen that induces the autoimmune response has not been identified yet. Some candidate autoantigens are myelin basic protein (MBP), proteolipidprotein (PLP) and myelin oligodendrocyte glycoprotein (MOG).[4] Of these proteins, MOG was found in animal models to be critical for the induction of demyelinating disease.[5,6] In these studies, some regions of this protein have been found to induce strong immune responses, especially the peptide spanning residues 35-55 (MOG_{35-55}).[7,8]

One key area of active research in MS is that of post-translational modification of myelin proteins, in particular citrullination. Citrullination is the enzymatic deimidation of arginine, converting the guanidine function into a urea function. This reaction is carried out by a group of enzymes called the peptidyl arginine deimidases (PADs).[9] Hypercitrullination of MBP,[10,11] as well as a general increase in citrullinated proteins in brain samples[12] have been shown to be hallmarks of MS. Therefore, the biophysical and biochemical effects of citrullination on MPB and other myelin proteins, like MOG, is an area of active research.

Recently, the observation was made that the previously mentioned immunodominant peptide of murine MOG, $mMOG_{35-55}$, showed amyloid-like aggregation behavior after posttranslational citrullination.[13] Amyloid-like aggregation starts with a peptide (or protein) folding into a stable, β-sheet rich conformation. These structures can then associate with each other, forming oligomers and finally polymeric fibrils. This process is thermodynamically favorable, and formed fibrils have been shown to nucleate further amyloid formation, creating a positive feedback loop that drives the process towards further aggregation.[14]

This observation may place MS into the constantly growing class of amyloid diseases. This category contains many other incurable neurodegenerative diseases including Alzheimer's and Parkinson's disease. In these diseases, the formation of amyloids, from the Aβ peptide in Alzheimer's disease[15] and the protein α-synuclein in Parkinson's disease[16], produce fibrils that appear to be involved in disease progression. While amyloid-like aggregates have not been shown inside MS patient brain autopsies, the potential involvement of amyloids in MS pathology and disease progression is an exciting line of inquiry. Specifically, the speculative involvement of an amyloidogenic process might explain some of the features of progressive MS, as well as the switch from RRMS to SPMS, both of which are yet poorly understood.[17]

However, the above-described research on MOG_{35-55} aggregation was conducted using a peptide derived from the murine sequence of MOG. MOG, and specifically the immunodominant regions involved, are highly conserved between species. While this is a helpful feature for animal experiments, some single amino acid polymorphisms are present and their effects need to be considered. Specifically, the murine and human sequence of the MOG_{35-55} peptide differs by one residue, with the murine Ser_{42} residue substituted for Pro in

humans (Figure 1). MOGs of other commonly used laboratory animals (*i.e.*, rats and common marmosets) also feature a Ser$_{42}$ residue. It is not unlikely that the switch from Ser to Pro drives human MOG$_{35-55}$ to behave different from that of these animal models.

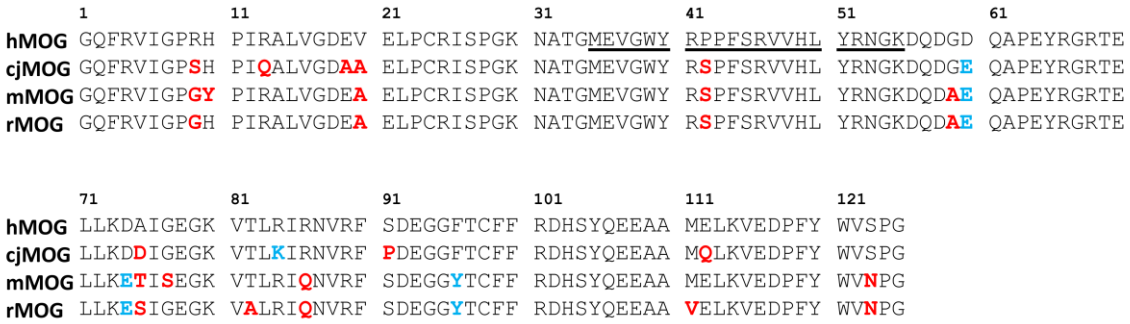

Figure 1. Amino acid sequence of the extracellular part (AAs 1-125) of Myelin Oligodendrocyte Glycoprotein (MOG) for human (hMOG), *Callithrix jacchus* or common marmoset (cjMOG), mice (mMOG) and rat (rMOG). Residues that are mutated compared to the human protein are marked red, while minor, highly similar, mutations are marked in blue. The immunodominant portion, MOG$_{35-55}$, is underlined.

In this chapter, the amyloidogenic properties of citrullinated human and murine MOG$_{35-55}$ peptides are compared to each other. To investigate the sensitivity of the aggregation of citrullinated MOG$_{35-55}$ peptides to variation on position 42, some further modifications on this position were also screened, that covered the intermediate chemical space between the mouse and human MOG-peptides. Finally, the immunological consequences of these Ser-to-Pro modifications were evaluated using an earlier described B-cell cross-presentation assay in the marmoset.[18]

Results and discussion

To investigate whether amyloid-like aggregation is unique to the mouse peptide, hMOG$_{35-55}$ peptides bearing the same citrullination patterns as the strongest aggregating mouse peptides, hMOG$_{35-55}$-Cit$_{41,46}$ and hMOG$_{35-55}$-Cit$_{46,52}$, were synthesized. The hMOG$_{35-55}$ peptide, bearing no Arg-to-Cit substitutions, was also synthesized as a control. All peptides were synthesized on Tentagel S RAM resin for its ease of synthesis, yielding the desired C-terminally amidated peptides, as previously reported in Chapter 2 and by Araman *et al.*[13]

Next, MOG$_{35-55}$ peptides where Ser$_{42}$ was replaced with alanine, threonine, or the unnatural amino acid L-aminobutyric acid (Abu), structurally close analogues of serine, were synthesized. These isosteres of serine were hypothesized to show comparable amyloid-like aggregation and were postulated to reveal something about the importance of position 42 for aggregation. Furthermore, proline hydroxylation,[19] an oxidative modification of proline that introduces a hydroxyl group onto the proline pyrrolidine ring, was considered as a potential modifier of the aggregation of the human peptide, since the hydroxy function of serine could be critical to the aggregation. In order to test this hypothesis, peptides replacing Pro$_{42}$ or Pro$_{43}$ with 4-

hydroxyproline were also synthesized. A complete overview of all the synthesized peptides, together with a qualitative indication of their aggregation propensity and the chemical yield after Fmoc-SPPS synthesis and RP-HPLC purification, is given in Table 1.

Table 1. Overview of all synthesized peptides. In every peptide sequence the amino acids changed from the human sequence hMOG$_{35-55}$ are highlighted in boldface. [a] explanation of aggregation symbols: -, no aggregation at all concentrations; +, slow aggregation at some concentrations; ++, rapid aggregation at some concentrations, +++, rapid concentration at all concentrations; [b] synthesis was previously described in Araman *et al.*[13]

Name	Sequence	Aggregation[a]	Yield (%)
hMOG$_{35-55}$	MEVGWYRPPFSRVVHLYRNGK-NH_2	-	26
hMOG$_{35-55}$-Cit$_{41,46}$	MEVGWY***Cit***PPFS***Cit***VVHLYRNGK-NH_2	-	12
hMOG$_{35-55}$-Cit$_{46,52}$	MEVGWYRPPFS***Cit***VVHLY***Cit***NGK-NH_2	-	22
mMOG$_{35-55}$	MEVGWYR**S**PFSRVVHLYRNGK-NH_2	-	-[b]
mMOG$_{35-55}$-Cit$_{41,46}$	MEVGWY***Cit*****S**PFS***Cit***VVHLYRNGK-NH_2	+++	-[b]
mMOG$_{35-55}$-Cit$_{46,52}$	MEVGWYR**S**PFS***Cit***VVHLY***Cit***NGK-NH_2	+++	-[b]
MOG$_{35-55}$-Ala$_{42}$-Cit$_{41,46}$	MEVGWY***Cit*****A**PFS***Cit***VVHLYRNGK-NH_2	-	24
MOG$_{35-55}$-Ala$_{42}$-Cit$_{46,52}$	MEVGWYR**A**PFS***Cit***VVHLY***Cit***NGK-NH_2	++	21
MOG$_{35-55}$-Thr$_{42}$-Cit$_{41,46}$	MEVGWY***Cit*****T**PFS***Cit***VVHLYRNGK-NH_2	-	35
MOG$_{35-55}$-Thr$_{42}$-Cit$_{46,52}$	MEVGWYR**T**PFS***Cit***VVHLY***Cit***NGK-NH_2	-	16
MOG$_{35-55}$-Abu$_{42}$-Cit$_{41,46}$	MEVGWY***CitAbu***PFS***Cit***VVHLYRNGK-NH_2	++	30
MOG$_{35-55}$-Abu$_{42}$-Cit$_{46,52}$	MEVGWYR***Abu***PFS***Cit***VVHLY***Cit***NGK-NH_2	-	38
MOG$_{35-55}$-Hyp$_{42}$-Cit$_{41,46}$	MEVGWY***CitHyp***PFS***Cit***VVHLYRNGK-NH_2	-	13
MOG$_{35-55}$-Hyp$_{42}$-Cit$_{46,52}$	MEVGWYR***Hyp***PFS***Cit***VVHLY***Cit***NGK-NH_2	-	30
hMOG$_{35-55}$-Hyp$_{43}$-Cit$_{41,46}$	MEVGWY***Cit***P***Hyp***FS***Cit***VVHLYRNGK-NH_2	-	27
hMOG$_{35-55}$-Hyp$_{43}$-Cit$_{46,52}$	MEVGWYRP***Hyp***FS***Cit***VVHLY***Cit***NGK-NH_2	-	23

The formation of amyloid like aggregates was quantified using the fluorogenic dye Thioflavin T,[20] as described in Chapter 2. This dye strongly increases its fluorescence upon binding to the typical cross-beta sheet-like structures that are present in amyloid-like aggregates. This allowed for the study of the kinetics of aggregate formation. The peptides were incubated at 37°C in a sodium acetate buffer at pH 5, conditions previously determined to be optimal for mMOG$_{35-55}$-Cit$_{41,46}$ and mMOG$_{35-55}$-Cit$_{46,52}$, (as these peptides are produced after uptake in the lysosome, where the environment is acidic) for up to 16 hours while the amyloid aggregation was followed by measuring the increase of the ThT fluorescent signal, as compared to a sample containing no peptide. As expected, neither hMOG$_{35-55}$ (Figure 2A) nor mMOG$_{35-55}$ (Figure 2B) showed amyloid-like aggregation under these conditions. Surprisingly, while mMOG$_{35-55}$-Cit$_{41,46}$ (Figure 2D) and mMOG$_{35-55}$-Cit$_{46,52}$ (Figure 2F) peptides showed clear increase in ThT signal over time as expected, this effect was absent for the hMOG$_{35-55}$-Cit$_{41,46}$ (Figure 2C) and for hMOG$_{35-55}$-Cit$_{46,52}$ (Figure 2E) peptides. This indicates that these peptides, unlike their murine counterparts, are *not* amyloidogenic.

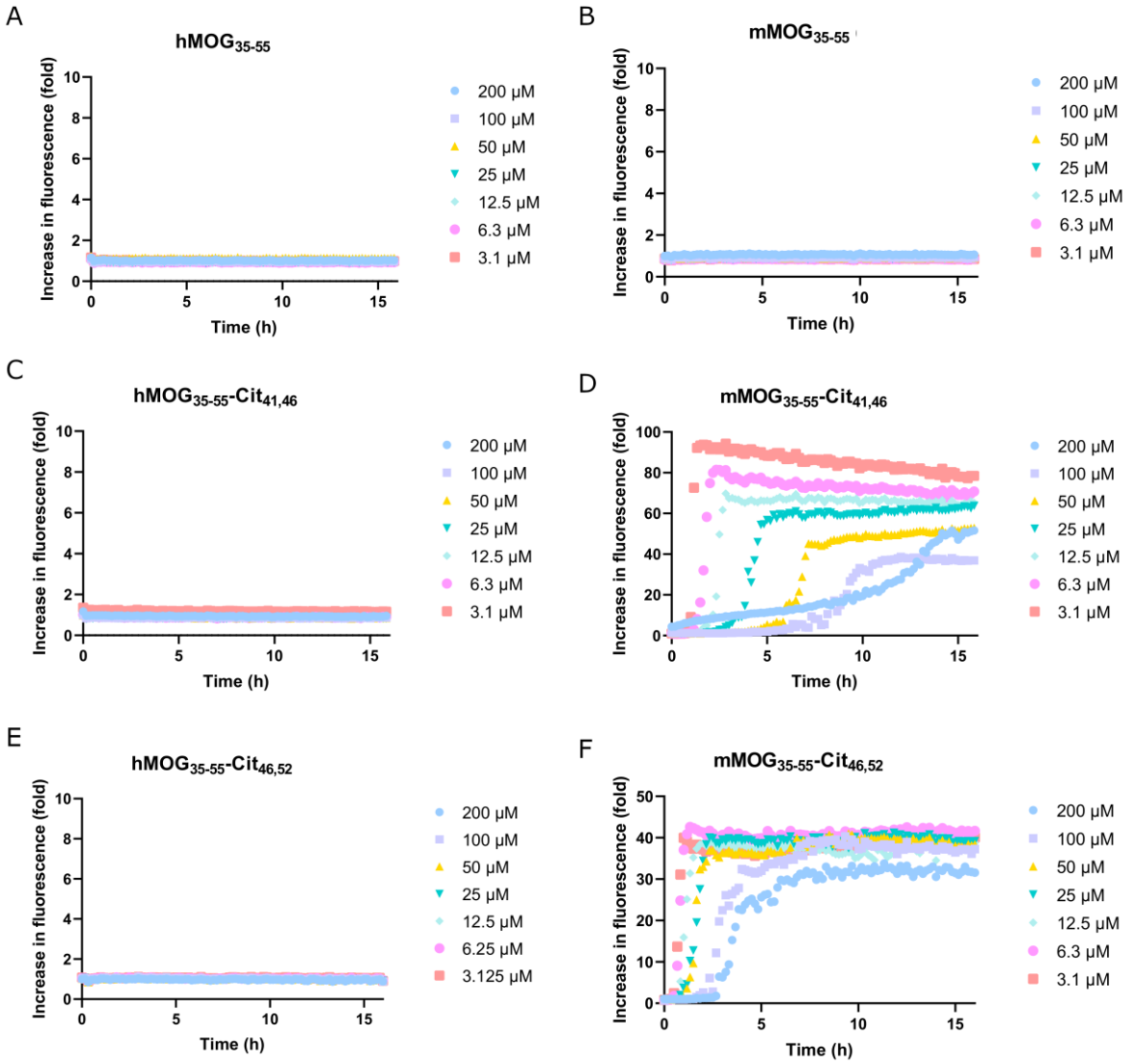

Figure 2. A-F) ThT aggregation assays showing the aggregation properties of hMOG$_{35-55}$ and mMOG$_{35-55}$ and their citrullinated variants at pH=5 (20 mM NaOAc buffer) and 37°C.

To assess whether the hMOG peptides had any propensity to aggregate at all, a seeding experiment was performed by which solutions of the human peptide were seeded with aggregates of mMOG$_{35-55}$-Cit$_{46,52}$. To this end, 200 µL of a 40 µM mMOG$_{35-55}$-Cit$_{46,52}$ solution in pH 5 NaOAc buffer was incubated at 37°C for 24 hours, followed by centrifugation at 20,000 g for 30 minutes. After discarding the supernatant, the seeds were homogenized in 200 µL buffer and co-incubated with either hMOG$_{35-55}$-Cit$_{41,46}$ or hMOG$_{35-55}$-Cit$_{46,52}$. No aggregation was observed in these experiments, indicating that nucleation is not the missing factor that can induce aggregation of citrullinated hMOG$_{35-55}$ peptides.

Next, the series of peptides containing the close analogues of serine, that is alanine, threonine and aminobutyric acid, were similarly evaluated using the ThT assay (Figure 3).

Firstly, alanine modification was assessed, where Ser$_{42}$ was substituted by an alanine residue. In this series, MOG$_{35-55}$-Ala$_{42}$-Cit$_{41,46}$ showed little increase in ThT fluorescence over 16h

(Figure 3A), whereas MOG_{35-55}-Ala_{42}-$Cit_{46,52}$ did show a clear increase in ThT signal (Figure 3B). However, when compared to the original serine containing peptide, $mMOG_{35-55}$-$Cit_{46,52}$, the aggregation was slower. This difference in time of onset was obtained by fitting a sigmoidal aggregation curve to the data obtained at a concentration of 3.1, 6.3 and 12.5 µM.[21] However, the quality of the fit was poor, indicating that the alanine substituted peptide does not fit the sigmoidal aggregation model well, making calculations of the differences of the rate of aggregation complicated. However, with these limitations kept in mind, an t_{50} (time to reaching 50% of maximum fluorescence) of 6.1 ± 0.2 hours was obtained for this peptide at 6.3 µM concentration. This gives a Δt_{50} of 5.3 hours compared to $mMOG_{35-55}$-$Cit_{46,52}$, for which a t_{50} of 0.79 ± 0.012 hours was found at the same concentration.

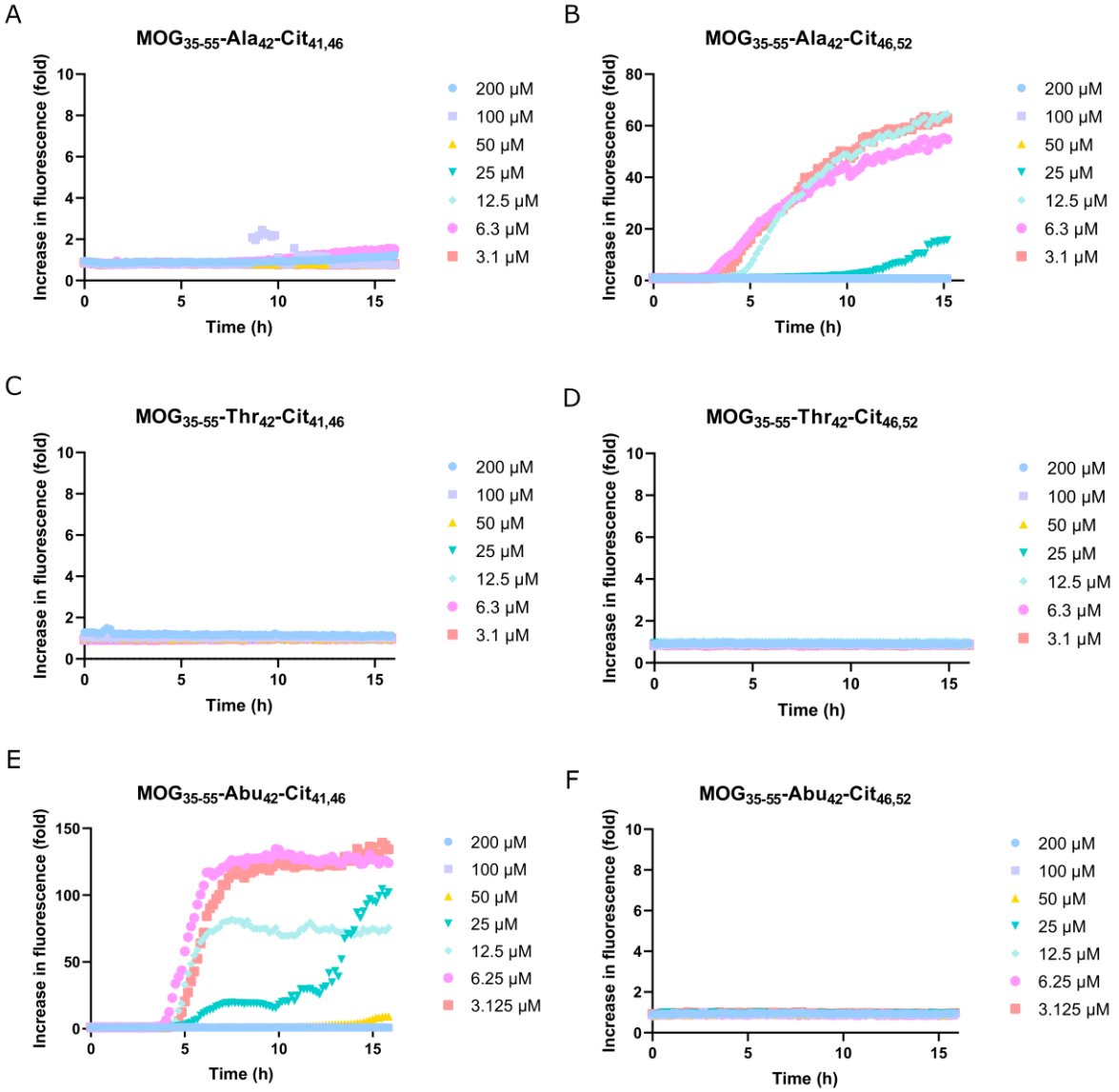

Figure 3. ThT aggregation assays showing the aggregation properties of MOG_{35-55}-$Cit_{41,46}$ and MOG_{35-55}-$Cit_{46,52}$ when Ser_{42} is replaced with either alanine (A, B), threonine (C, D), L-2-aminobutyric acid (Abu) (E, F)

The peptides with the Ser-to-Thr substitution at position 42, MOG_{35-55}-Thr_{42}-$Cit_{41,46}$ and MOG_{35-55}-Thr_{42}-$Cit_{46,52}$, were considered next. These peptides, again showed no increase in ThT fluorescence for the entire duration of the measurement (Figures 3C&3D).

The peptides in which Ser was substituted for the unnatural amino acid L-aminobutyric acid showed the opposite effect on aggregation from the alanine containing peptide was observed, as MOG_{35-55}-Abu_{42}-$Cit_{41,46}$ (Figure 3E) showed amyloid-like aggregation behavior in the ThT assay while its counterpart MOG_{35-55}-Abu_{42}-$Cit_{46,52}$ (Figure 3F) did not. The citrullinated $hMOG_{35-55}$ peptides containing 4-hydroxyproline (Hyp) in place of Pro_{42} and/or Pro_{43} were evaluated as these peptides represent a biologically accessible hybrid between the human and the mouse peptides (i.e. containing both a hydroxyl-functionality and a proline). None of these showed an increase in ThT fluorescence after 16 hours (Figure 4). This indicates that simple oxidation of proline to hydroxyproline is insufficient to turn a nonaggregating peptide into an aggregating one.

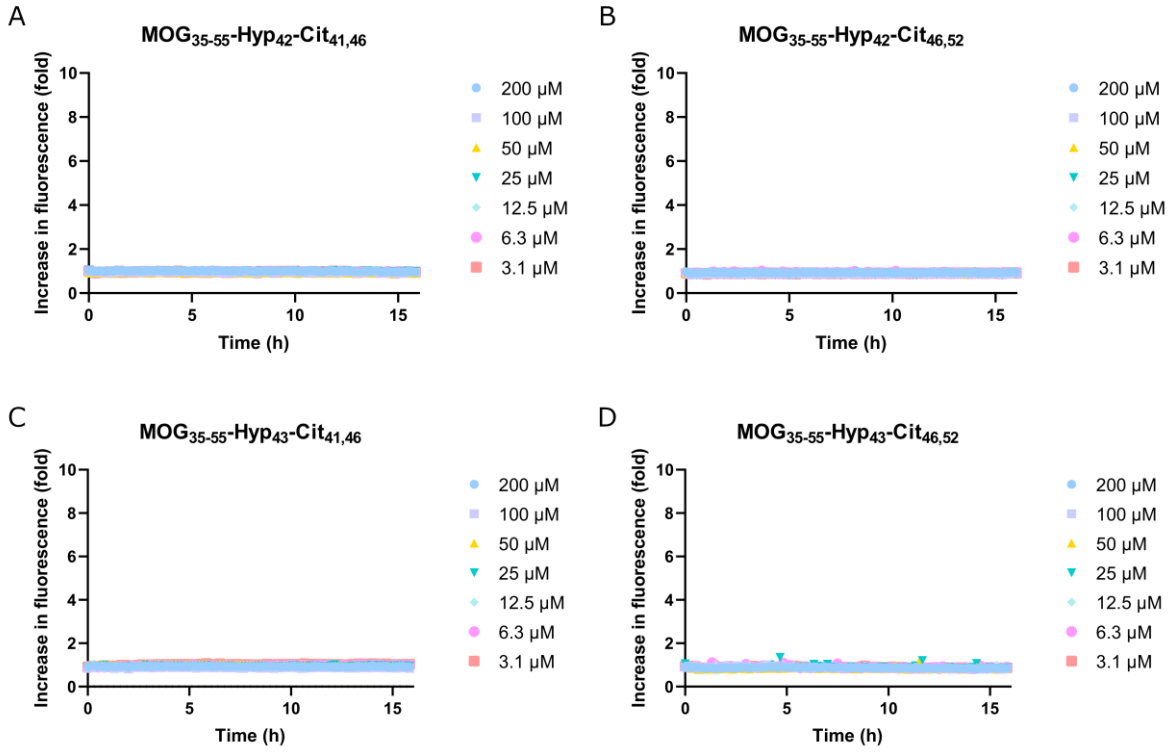

Figure 4. ThT aggregation assays showing the aggregation properties of citrullinated $hMOG_{35-55}$ peptides hydroxylated on either Pro_{42} (A, B) or Pro_{43} (C, D)

In conclusion, it seems that the primary hydroxyl functionality of serine is of key importance to this aggregation process as none of the peptides containing an aliphatic amino acid instead of serine displayed the same level of aggregation. The lack of aggregation seen with amino acids bearing a secondary alcohol, as well as the erratic aggregation of the alkylic amino acids could imply that both the size of the sidechain and the serine hydroxyl group have key roles in the aggregation process.

These findings could have great impact on the interpretation of immunological experiments carried out with these peptides in animal-model studies. One of these models, and one of the more refined animal models of multiple sclerosis-like neuroinflammation and neurodegeneration, is the experimental autoimmune encephalomyelitis (EAE) model in the common marmoset (*Callitrix jacchus*) developed by the 't Hart group. In this model, in contrast to many of the earlier murine models, immunization with the $hMOG_{35-55}$ peptide, in the absence of any immune adjuvant, induces severe neurological inflammation and impairment.[18,22] This finding underlines the great immune stimulating potential of this short MOG peptide.

Further characterization of this model found a critical role for B-cells as antigen presenting cells for the activation of $CD8^+$ T-cells. Surprisingly, it was found that the immunodominant epitope $hMOG_{40-48}$ was presented via the non-classical MHC I molecule Caja-E, a close marmoset analogue to the human HLA-E complex.[18] In an *in vitro* assay using cells derived from these monkeys, it had previously been shown that the aggregating citrullinated peptides $mMOG_{35-55}$-$Cit_{41,46}$ and $mMOG_{35-55}$-$Cit_{41,46}$, in contrast to non-citrullinated $mMOG_{35-55}$, did *not* induce T-cell proliferation, instead displaying cytotoxicity.[13]

An important unanswered biological question stemming from this was whether the changes in aggregation of citrullinated $mMOG_{35-55}$ between mouse and human sequences affected T-cell responses against the dominant MHC-I-restricted epitopes contained within these sequences. With the remarkable difference in amyloidogenic potential between the human and murine peptides now known, it was next investigated what, if any, effect this has on the cross-presentation potential of these peptides.

To this end, T-cell activation by the different human and murine MOG_{35-55} peptides was evaluated. For this assay, cells isolated from the axillary lymph node (ALN) of marmosets immunized with $hMOG_{34-56}$ were utilized, as reported previously.[13,23] Briefly, EBV-infected marmoset B-lymphoblastoid cells (BLCs) were lethally irradiated and incubated with different concentration (10, 3 and 1 µM) of the peptides for 1 hour. After this incubation period, freshly thawed marmoset ALN cells were added to the BLC culture and co-cultured for 48 hours and the proliferation of the lymphocyte cells was determined via an [^{3}H]thymidine incorporation assay. From this assay a stimulation index (SI, ratio of proliferation of treated cells versus untreated control) was calculated, and a SI > 2 was considered T-cell activation. The experiment was carried out with cells isolated from three different marmosets and the individual responses as well as the mean response were plotted in Figure 5.

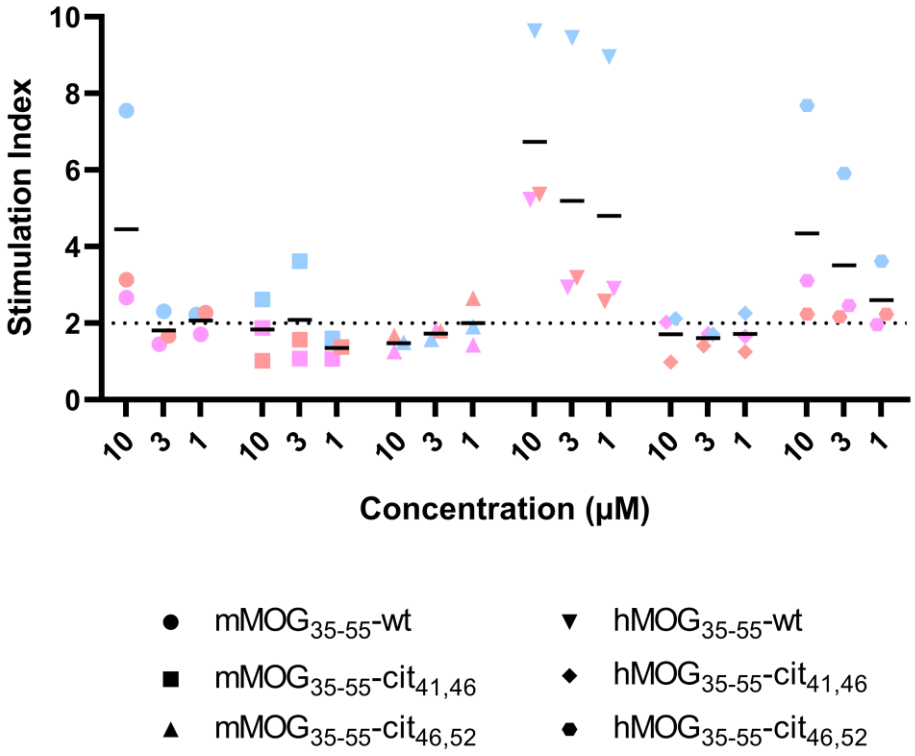

Figure 5. B-cells isolated from rhMOG immunized marmosets where stimulated with different peptides at the indicated concentrations for 1 hours. T-cells were added and proliferation was measured using a [^{3}H]thymidine incorporation assays. A stimulation index (ratio of proliferation for stimulated T-cells versus unstimulated control, SI) was plotted for each condition and SI > 2 was taken as the cut-off for T-cell activation. The experiment was carried out using material from three different animals (N=3), with the individual responses shown as three distinct colors.

A strong response against $hMOG_{35-55}$ was observed at all concentrations tested, which was expected as this was the immunogen used to immunize the marmosets. The peptide derived from the murine (and also marmoset) sequence, $mMOG_{35-55}$ also induced a strong proliferation at the highest tested concentration (10 µM). The citrullinated human peptide $hMOG_{35-55}$-$Cit_{46,52}$ produced a strong increase in T-cell proliferation, while the murine counterpart $mMOG_{35-55}$-$Cit_{46,52}$ shows no proliferation. Finally, neither $mMOG_{35-55}$-$Cit_{41,46}$ nor $hMOG_{35-55}$-$Cit_{41,46}$ produced a T-cell response in this assay. While previous work had already indicated immunological differences between human and murine MOG_{35-55} using a murine system,[24] this striking difference of T-cell activation between $mMOG_{35-55}$-$Cit_{46,52}$ and $hMOG_{35-55}$-$Cit_{46,52}$ was unknown.

Conclusion

The role of citrullination in both MS and EAE is currently poorly understood. While evidence exists for an increase of citrullination of the key myelin protein Myelin Basic Protein (MBP)[25] as well as a general increase in protein citrullination in white matter[26] in MS patients, citrullination of MOG itself has never been directly detected. However, in the animal model of MS, EAE, MOG is the most commonly studied autoantigen, and the effect of citrullination on the key antigenic peptide MOG_{35-55} has been studied extensively.[27–30]

The recently described aggregation behavior of citrullinated $mMOG_{35-55}$[13] opened up a new avenue for MOG mediated disease progression in MS, where the aggregation of citrullinated peptide could potentially directly induce neurodegeneration once sufficient levels of citrullination are achieved. However, the findings in this chapter show that the aggregation of citrullinated MOG_{35-55} is inherent only to the peptides containing serine on position 42, a polymorphism that is present in many of the commonly studied laboratory animals (mice, rats, common marmosets), but is replaced by proline in the human sequence of MOG. This one amino acid change renders the peptide completely resistant to amyloid like aggregation under the conditions that were optimal for the murine peptides.

In order to better understand the large effect this single amino acid substitution has on the peptide properties, a series of single amino acid substitutions were synthesized and screened for their aggregation behavior. The results obtained here indicate that serine is critical for the observed effect, with all amino acid substitutions tested producing either a far weaker aggregating peptide or, in most cases, a non-aggregating peptide.

The aforementioned previous study on the aggregating citrullinated murine peptides had also shown non-immunogenic properties of these peptides in an EBV infected B-cell cross-presentation assay. Unexpectedly, one of the human citrullinated peptides tested here, $hMOG_{35-55}$-$Cit_{46,52}$, showed strong T-cell activation in the same assay, raising questions about the validity of the animal models for the study of the autoantigenic responses in MS. A potential explanation for the discrepancy in T-cell activation is the aggregation behavior of the murine peptide. The murine citrullinated peptide might form an insoluble aggregate either inside or outside of the cell, inhibiting both (productive) peptide processing and epitope presentation. It is currently unknown whether the aggregated forms of the murine peptides are resistant to degradation and how this influences antigen processing. However, one could speculate that the formed aggregates might prohibit production of the key epitope peptide, limiting T-cell activation in this way. Additionally, while not studied here, cytotoxicity of aggregated peptide towards T-cells has been put forward as a potential reason for lack of T-cell activation observed with the citrullinated $mMOG_{35-55}$ peptides.[13]

Taken together, more work is needed in validating multiple sclerosis animal models using myelin oligodendrocyte glycoprotein as a model autoantigen, especially when studying the effects of citrullination.

Experimental

General peptide synthesis

SPPS of peptides was carried out using manual synthesis on a 50 µmol on Tentagel S RAM resin (Rapp Polymere GmbH, Germany) when a C-terminal carboxamide was desired, or on chloro-(2'-chloro)-trityl (CTC) polystyrene resin when a C-terminal carboxylic acid was intended. Fmoc protected amino acids were purchased from either Novabiochem or Sigma-Aldrich. For the amino acids that require sidechain protection, the following protecting groups were used: tBu for Ser, Thr, Tyr and Hyp; OtBu for Asp and Glu; Trt for Asn, Gln and His; Boc for Lys and Trp; Pbf for Arg. To load the first amino acid onto CTC resin, 2 eq of the desired amino acid together with 5 eq of DiPEA dissolved in anhydrous DCM (1.25 mL) are added to the resin which was gently agitated overnight. The loaded resin was then washed with DCM and capped using a mixture of MeOH/DiPEA/DCM (2:1:17) for one hour. To extend the growing peptide chain, 5 eq of Fmoc-amino acid was mixed together with an equimolar quantity of 2-(6-Chloro-1-H-benzotriazole-1-yl)-1,1,3,3-tetramethylaminium hexafluorophosphate (HCTU) in DMF at an concentration of 0.5 M, followed by the addition of 10 eq of diisopropylethylamine (DiPEA) and preactivation for 2 minutes. Coupling reaction were carried out for 30-45 minutes. Fmoc deprotection was accomplished by repeated treatment with 20% piperidine in DMF (3 + 7 min). Global deprotection and resin cleavage of peptides was accomplished using a 95:2.5:2.5 mixture of TFA/TIS/H_2O for 3 hours, followed by precipitation from cold diethyl ether (1:9 ratio TFA to ether) and recovery of the precipitate by centrifugation. Crude, tryptophan containing peptides were dissolved in MilliQ water an lyophilized overnight in order to remove the residual carboxylate. Preparative reverse phase HPLC on a Waters AutoPurification system (eluent A: H_2O + 0.2% TFA; eluent B: ACN) with a preparative Gemini C18 column (5 µm, 150 x 21.2 mm) yielded the final products. Peptides were characterized using electrospray ionization mass spectrometry (ESI-MS) on a Thermo Finnigan LCQ Advantage Max LC-MS instrument with a Surveyor PDA plus UV detector on an analytical C18 column (Phenomenex, 3 µm, 110 Å, 50 mm × 4.6 mm) in combination with buffers A (H_2O), B (MeCN), and C (1% aq TFA). Quality of crude and purified peptides was evaluated with a linear gradient of 10-50% B with a constant 10% C over 10 minutes. Preparative reverse phase HPLC on a Waters AutoPurification system (eluent A: H_2O + 0.2% TFA; eluent B: ACN) with a preparative Gemini C18 column (5 µm, 150 x 21.2 mm) yielded the final products.

Table of synthesized peptides

Table 2. Overview of all synthesized peptides. [a] synthesis was previously described in Araman *et al.*[13]

Name	Sequence	Expected mass [M+2H]	Found mass [M+2H]	Yield (%)
$mMOG_{35-55}$	MEVGWYRSPFSRVVHLYRNGK-NH_2	-	-	-[a]
$hMOG_{35-55}$	MEVGWYRPPFSRVVHLYRNGK-NH_2	1295.7	1296.3	25.6
$hMOG_{35-55}$-$Cit_{41,46}$	MEVGWY*Cit*PPFS*Cit*VVHLYRNGK-NH_2	1296.5	1297.3	12.4
$hMOG_{35-55}$-$Cit_{46,52}$	MEVGWYRPPFS*Cit*VVHLY*Cit*NGK-NH_2	1296.5	1297.4	22.4
$mMOG_{35-55}$-$Cit_{41,46}$	MEVGWY*Cit*SPFS*Cit*VVHLYRNGK-NH_2	-	-	-[a]
$mMOG_{35-55}$-$Cit_{46,52}$	MEVGWYRSPFS*Cit*VVHLY*Cit*NGK-NH_2	-	-	-[a]

MOG$_{35-55}$-Ala$_{42}$-Cit$_{41,46}$	MEVGWY*Cit*APFS*Cit*VVHLYRNGK-NH_2	1283.7	1284.2	24.2
MOG$_{35-55}$-Ala$_{42}$-Cit$_{46,52}$	MEVGWYRAPFS*Cit*VVHLY*Cit*NGK-NH_2	1283.7	1284.2	21.1
MOG$_{35-55}$-Thr$_{42}$-Cit$_{41,46}$	MEVGWY*Cit*TPFS*Cit*VVHLYRNGK-NH_2	1298.7	1299.1	34.9
MOG$_{35-55}$-Thr$_{42}$-Cit$_{46,52}$	MEVGWYRTPFS*Cit*VVHLY*Cit*NGK-NH_2	1298.7	1299.1	15.8
MOG$_{35-55}$-Abu$_{42}$-Cit$_{41,46}$	MEVGWY*CitAbu*PFS*Cit*VVHLYRNGK-NH_2	1290.7	1291.2	30.2
MOG$_{35-55}$-Abu$_{42}$-Cit$_{46,52}$	MEVGWYR*Abu*PFS*Cit*VVHLY*Cit*NGK-NH_2	1290.7	1291.3	38.3
MOG$_{35-55}$-Hyp$_{42}$-Cit$_{41,46}$	MEVGWY*CitHyp*PFS*Cit*VVHLYRNGK-NH_2	1304.7	1305.3	13.0
MOG$_{35-55}$-Hyp$_{42}$-Cit$_{46,52}$	MEVGWYR*Hyp*PFS*Cit*VVHLY*Cit*NGK-NH_2	1304.7	1305.1	30.0
hMOG$_{35-55}$-Hyp$_{43}$-Cit$_{41,46}$	MEVGWY*Cit*P*Hyp*FS*Cit*VVHLYRNGK-NH_2	1304.7	1305.1	27.1
hMOG$_{35-55}$-Hyp$_{43}$-Cit$_{46,52}$	MEVGWYRP*Hyp*FS*Cit*VVHLY*Cit*NGK-NH_2	1304.7	1305.3	23.4

ThT Fluorescence Aggregation Assays

Aggregation assays were carried out in 96-well plate format using a Infinite M1000 Pro Tecan plate reader. The excitation and emission wavelengths were set to 444 nm and 485 nm respectively, with a bandwidth of 10 nm. For each peptide under investigation, a 200 µM stock in sodium ascorbate buffer (20 mM, pH=5) was prepared and from this stock a serial diluted was made using the same buffer. Of these solutions, 199 µL of peptide stock was added into a well and mixed with 1 µL of 1 mM Thioflavin T stock solution, prepared in the same NaOAc buffer, for a final dye concentration of 5 µM. Every concentration of peptide was measured in triplicate. The plate was kept at 37°C and the fluorescence was measured every ten minutes for 16 hours. The fluorescence was normalized against a well containing 5 µM Thioflavin T in buffer that was measured alongside the assay.

T-cell Culture Assay

Mononuclear cells (MNC) were isolated from the axillary lymph node (ALN) from three adult common marmosets (*Callithrix jacchus*). These animals were used in EAE studies, to induce EAE the animals were immunised with MOG_{34-56} (Cambridge research biochemicals Ltd.) emulsified in IFA. EBV infected marmoset B-cells (BCLs) were used as antigen presenting cells.

For the proliferation assay the marmoset BCLs were collected and washed with PBS and irradiated with 70Gy in RPMI (Gibco) without FCS. BCLs were plated in 96-well round bottom plates (Greiner) at the concentration of $1{\cdot}10^3$ cells/well and incubated for 1H in an incubator with 5% CO_2 and 37°C with different concentration of the peptides (1 µM, 3 µM and 10 µM), the medium was used as a negative control. After 1 hour, thawed MNC were added to the BCLs at a concentration of $1{\cdot}10^5$ cells/well. After 48 hour 25µL of [methyl-3H] thymidine (0.1 mCi/mL stock; PerkinElmer) was added. 18 hour later the cells were harvested using a Filtermate Harvester (PerkinElmer) on a microfilter plate. When the plate had dried, 25µL of Ultima Gold™ (PerkinElmer) was added and measured on a MicroBeta2 counter (PerkinElmer).

References

(1) Thompson, A. J.; Baranzini, S. E.; Geurts, J.; Hemmer, B.; Ciccarelli, O. Multiple Sclerosis. *The Lancet*. Lancet Publishing Group April 21, 2018, pp 1622–1636. https://doi.org/10.1016/S0140-6736(18)30481-1.

(2) Dendrou, C. A.; Fugger, L.; Friese, M. A. Immunopathology of Multiple Sclerosis. *Nat. Rev. Immunol.* **2015**, *15* (9), 545–558. https://doi.org/10.1038/nri3871.

(3) Milo, R.; Kahana, E. Multiple Sclerosis: Geoepidemiology, Genetics and the Environment. *Autoimmunity Reviews*. Elsevier March 1, 2010, pp A387–A394. https://doi.org/10.1016/j.autrev.2009.11.010.

(4) Fraussen, J.; Claes, N.; de Bock, L.; Somers, V. Targets of the Humoral Autoimmune Response in Multiple Sclerosis. *Autoimmun. Rev.* **2014**, *13* (11), 1126–1137. https://doi.org/10.1016/j.autrev.2014.07.002.

(5) McFarland, H. I.; Lobito, A. A.; Johnson, M. M.; Nyswaner, J. T.; Frank, J. A.; Palardy, G. R.; Tresser, N.; Genain, C. P.; Mueller, J. P.; Matis, L. A.; Lenardo, M. J. Determinant Spreading Associated with Demyelination in a Nonhuman Primate Model of Multiple Sclerosis. *J. Immunol.* **1999**, *162* (4), 2384–2390.

(6) Smith, P. A.; Heijmans, N.; Ouwerling, B.; Breij, E. C.; Evans, N.; van Noort, J. M.; Plomp, A. C.; Delarasse, C.; Hart, B.; Pham-Dinh, D.; Amor, S. Native Myelin Oligodendrocyte Glycoprotein Promotes Severe Chronic Neurological Disease and Demyelination in Biozzi ABH Mice. *Eur. J. Immunol.* **2005**, *35* (4), 1311–1319. https://doi.org/10.1002/eji.200425842.

(7) Bernard, C. C. A.; Johns, T. G.; de Rosbo, N. K.; Ichikawa, M. A Peptide from Myelin Oligodendrocyte Glycoprotein That Induces Demyelinating Encephalomyelitis Resembling Multiple Sclerosis. *J. Neuroimmunol.* **1994**, *54* (1–2), 153. https://doi.org/10.1016/0165-5728(94)90266-6.

(8) Mendel, I.; Rosbo, N. K. de; Ben-Nun, A. Delineation of the Minimal Encephalitogenic Epitope within the Immunodominant Region of Myelin Oligodendrocyte Glycoprotein: Diverse Vβ Gene Usage by T Cells Recognizing the Core Epitope Encephalitogenic for T Cell Receptor Vβb and T Cell Receptor Vβa H-2b Mice. *Eur. J. Immunol.* **1996**, *26* (10), 2470–2479. https://doi.org/10.1002/EJI.1830261030.

(9) Vossenaar, E. R.; Zendman, A. J. W.; Van Venrooij, W. J.; Pruijn, G. J. M. PAD, a Growing Family of Citrullinating Enzymes: Genes, Features and Involvement in Disease. *BioEssays*. John Wiley & Sons, Ltd November 1, 2003, pp 1106–1118. https://doi.org/10.1002/bies.10357.

(10) Wood, D. D.; Moscarello, M. A. The Isolation, Characterization, and Lipid-Aggregating Properties of a Citrulline Containing Myelin Basic Protein. *J. Biol. Chem.* **1989**, *264* (9), 5121–5127. https://doi.org/10.1016/s0021-9258(18)83707-3.

(11) Kim, J. K.; Mastronardi, F. G.; Wood, D. D.; Lubman, D. M.; Zand, R.; Moscarello, M. A. Multiple Sclerosis: An Important Role for Post-Translational Modifications of Myelin Basic Protein in Pathogenesis *. *Mol. Cell. Proteomics* **2003**, *2* (7), 453–462. https://doi.org/10.1074/MCP.M200050-MCP200.

(12) Luchicchi, A.; Hart, B.; Frigerio, I.; van Dam, A. M.; Perna, L.; Offerhaus, H. L.; Stys, P. K.; Schenk, G. J.; Geurts, J. J. G. Axon-Myelin Unit Blistering as Early Event in MS Normal Appearing White Matter. *Ann. Neurol.* **2021**, *89* (4), 711–725. https://doi.org/10.1002/ana.26014.

(13) Araman, C.; Van Gent, M. E.; Meeuwenoord, N. J.; Heijmans, N.; Marqvorsen, M. H. S.; Doelman, W.; Faber, B. W.; 't Hart, B. A.; Van Kasteren, S. I. Amyloid-like Behavior of Site-Specifically Citrullinated Myelin Oligodendrocyte Protein (MOG) Peptide Fragments inside EBV-Infected B-Cells Influences Their Cytotoxicity and Autoimmunogenicity. *Biochemistry* **2019**, *58* (6), 763–775. https://doi.org/10.1021/acs.biochem.8b00852.

(14) Harrison, R. S.; Sharpe, P. C.; Singh, Y.; Fairlie, D. P. Amyloid Peptides and Proteins in Review. In *Reviews of Physiology, Biochemistry and Pharmacology*; Amara, S. G., Bamberg, E., Fleischmann, B., Gudermann, T., Hebert, S. C., Jahn, R., Lederer, W. J., Lill, R., Miyajima, A., Offermanns, S., Zechner, R., Eds.; Springer Berlin Heidelberg: Berlin, Heidelberg, 2007; pp 1–77. https://doi.org/10.1007/112_2007_0701.

(15) Chen, G. F.; Xu, T. H.; Yan, Y.; Zhou, Y. R.; Jiang, Y.; Melcher, K.; Xu, H. E. Amyloid Beta: Structure, Biology and Structure-Based Therapeutic Development. *Acta Pharmacologica Sinica*. Nature Publishing Group July 17, 2017, pp 1205–1235. https://doi.org/10.1038/aps.2017.28.

(16) Zhang, G.; Xia, Y.; Wan, F.; Ma, K.; Guo, X.; Kou, L.; Yin, S.; Han, C.; Liu, L.; Huang, J.; Xiong, N.; Wang, T. New Perspectives on Roles of Alpha-Synuclein in Parkinson's Disease. *Front. Aging Neurosci.* **2018**, *10*, 370. https://doi.org/10.3389/FNAGI.2018.00370/BIBTEX.

(17) Correale, J.; Gaitán, M. I.; Ysrraelit, M. C.; Fiol, M. P. Progressive Multiple Sclerosis: From Pathogenic Mechanisms to Treatment. *Brain* **2017**, *140* (3), 527–546. https://doi.org/10.1093/brain/aww258.

(18) Jagessar, S. A.; Heijmans, N.; Blezer, E. L. A.; Bauer, J.; Blokhuis, J. H.; Wubben, J. A. M.; Drijfhout, J. W.; van den Elsen, P. J.; Laman, J. D.; Hart, B. A. '. Unravelling the T-Cell-Mediated Autoimmune Attack on CNS Myelin in a New Primate EAE Model Induced with MOG 34-56 Peptide in Incomplete Adjuvant. *Eur. J. Immunol.* **2012**, *42* (1), 217–227. https://doi.org/10.1002/eji.201141863.

(19) Zurlo, G.; Guo, J.; Takada, M.; Wei, W.; Zhang, Q. New Insights into Protein Hydroxylation and Its Important Role in Human Diseases. *Biochim. Biophys. Acta - Rev. Cancer* **2016**, *1866* (2), 208–220. https://doi.org/10.1016/j.bbcan.2016.09.004.

(20) Biancalana, M.; Koide, S. Molecular Mechanism of Thioflavin-T Binding to Amyloid Fibrils. *Biochimica et Biophysica Acta - Proteins and Proteomics*. Elsevier July 1, 2010, pp 1405–1412. https://doi.org/10.1016/j.bbapap.2010.04.001.

(21) Sabareesan, A. T.; Udgaonkar, J. B. Amyloid Fibril Formation by the Chain B Subunit of Monellin Occurs by a Nucleation-Dependent Polymerization Mechanism. *Biochemistry* **2014**, *53* (7), 1206–1217. https://doi.org/10.1021/bi401467p.

(22) Jagessar, S. A.; Kap, Y. S.; Heijmans, N.; Van Driel, N.; Van Straalen, L.; Bajramovic, J. J.; Brok, H. P. M.; Blezer, E. L. A.; Bauer, J.; Laman, J. D.; 'T Hart, B. A. Induction of Progressive Demyelinating Autoimmune Encephalomyelitis in Common Marmoset Monkeys Using MOG34-56 Peptide in Incomplete Freund Adjuvant. *J. Neuropathol. Exp. Neurol.* **2010**, *69* (4), 372–385. https://doi.org/10.1097/NEN.0b013e3181d5d053.

(23) Jagessar, S. A.; Heijmans, N.; Blezer, E. L. A.; Bauer, J.; Weissert, R.; 't Hart, B. A. Immune Profile of an Atypical EAE Model in Marmoset Monkeys Immunized with Recombinant Human Myelin Oligodendrocyte Glycoprotein in Incomplete Freund's Adjuvant. *J. Neuroinflammation* **2015**, *12* (1), 169. https://doi.org/10.1186/s12974-015-0378-5.

(24) Oliver, A. R.; Lyon, G. M.; Ruddle, N. H. Rat and Human Myelin Oligodendrocyte Glycoproteins Induce Experimental Autoimmune Encephalomyelitis by Different Mechanisms in C57BL/6 Mice. *J. Immunol.* **2003**, *171* (1), 462–468. https://doi.org/10.4049/JIMMUNOL.171.1.462.

(25) Moscarello, M. A.; Wood, D. D.; Ackerley, C.; Boulias, C. Myelin in Multiple Sclerosis Is Developmentally Immature. *J. Clin. Invest.* **1994**, *94* (1), 146–154. https://doi.org/10.1172/JCI117300.

(26) Faigle, W.; Cruciani, C.; Wolski, W.; Roschitzki, B.; Puthenparampil, M.; Tomas-Ojer, P.; Sellés-Moreno, C.; Zeis, T.; Jelcic, I.; Schaeren-Wiemers, N.; Sospedra, M.; Martin, R. Brain Citrullination Patterns and T Cell Reactivity of Cerebrospinal Fluid-Derived CD4+ T Cells in Multiple Sclerosis. *Front. Immunol.* **2019**, *0* (APR), 540. https://doi.org/10.3389/FIMMU.2019.00540.

(27) Carrillo-Vico, A.; Leech, M. D.; Anderton, S. M. Contribution of Myelin Autoantigen Citrullination to T Cell Autoaggression in the Central Nervous System. *J. Immunol.* **2010**, *184* (6), 2839–2846. https://doi.org/10.4049/jimmunol.0903639.

(28) Haanstra, K. G.; Wubben, J. A. M.; Jonker, M.; Hart, B. A. t. Induction of Encephalitis in Rhesus Monkeys Infused with Lymphocryptovirus-Infected B-Cells Presenting MOG34–56 Peptide. *PLoS One* **2013**, *8* (8), e71549. https://doi.org/10.1371/JOURNAL.PONE.0071549.

(29) Jagessar, S. A.; Holtman, I. R.; Hofman, S.; Morandi, E.; Heijmans, N.; Laman, J. D.; Gran, B.; Faber, B. W.; van Kasteren, S. I.; Eggen, B. J. L.; 't Hart, B. A. Lymphocryptovirus Infection of Nonhuman Primate B Cells Converts Destructive into Productive Processing of the Pathogenic CD8 T Cell Epitope in Myelin Oligodendrocyte Glycoprotein. *J. Immunol.* **2016**, *197* (4), 1074–1088. https://doi.org/10.4049/jimmunol.1600124.

(30) Morandi, E.; Jagessar, S. A.; 't Hart, B. A.; Gran, B. EBV Infection Empowers Human B Cells for Autoimmunity: Role of Autophagy and Relevance to Multiple Sclerosis. *J. Immunol.* **2017**, *199* (2), 435–448.